

Generalised Perspective Shape from Shading in Spherical Coordinates

Silvano Galliani^{1,2}, Yong Chul Ju^{1,3}, Michael Breuß¹, and Andrés Bruhn³

¹ Institute for Applied Mathematics and Scientific Computing,
BTU Cottbus, 03046 Cottbus, Germany
{galliani, ju, breuss}@tu-cottbus.de

² Institute of Geodesy and Photogrammetry,
ETH Zürich, 8093 Zürich, Switzerland
silvano.galliani@geod.baug.ethz.ch

³ Institute for Visualization and Interactive Systems,
University of Stuttgart, 70569 Stuttgart, Germany
bruhn@vis.uni-stuttgart.de

Abstract. In the last four decades there has been enormous progress in Shape from Shading (SfS) with respect to both modelling and numerics. In particular approaches based on advanced model assumptions such as perspective cameras and non-Lambertian surfaces have become very popular. However, regarding the positioning of the light source, almost all recent approaches still follow the simplest geometric configuration one can think of: The light source is assumed to be located exactly at the optical centre of the camera. In our paper, we refrain from this unrealistic and severe restriction. Instead we consider a much more general SfS scenario based on a perspective camera, where the light source can be positioned *anywhere* in the scene. To this end, we propose a novel SfS model that is based on a Hamilton-Jacobi equation (HJE) which in turn is formulated in terms of spherical coordinates. This particular choice of the modelling framework and the coordinate system comes along with two fundamental contributions: While on the modelling side, the spherical coordinate system allows us to derive a generalised brightness equation – a compact and elegant generalisation of the standard image irradiance equation to arbitrary configurations of the light source, on the numerical side, the formulation as Hamilton-Jacobi equation enables us to develop a specifically tailored variant of the fast marching (FM) method – one of the most efficient numerical solvers in the entire SfS literature. Results on synthetic and real-world data confirm our theoretical considerations. They clearly demonstrate the feasibility and efficiency of the generalised SfS approach.

Keywords: shape from shading, Hamilton-Jacobi equation, viscosity solution, fast marching, general light source configuration, spherical coordinates

1 Introduction

Since the early works of Rindfleisch [1] and Horn [2] more than four decades ago, *Shape from Shading (SfS)* is considered one of the key problems in computer vision.

Given the information about the reflectance of the surface and the position of the light source, its goal is to reconstruct the 3D depth of an object in a scene from a single 2D input image. In practice, SfS has a wide field of interesting applications. They range from classical large scale problems such as astronomy [1] or terrain reconstruction [3, 4] to challenging small scale tasks such as dentistry [5] or endoscopy [6–9].

In order to make both the modelling and the computation tractable, early SfS approaches relied on strongly simplified assumptions. Since these approaches were first used for large scale problems such as astronomy, they were typically based on a camera model with orthographic projection, a light source that illuminates the scene from infinity, as well as a physically incorrect light transport that neglects attenuation [2]. Not surprisingly, these early methods worked reasonably well in the case of large scale problems – the scenario they were designed for. However, if applied to tasks, where the distance of the camera to the object is small, such methods revealed a consistently poor performance in terms of reconstruction quality [10, 11]. Moreover, independent of the distance to the object, the corresponding mathematical models turned out to be severely ill-posed showing a strong dependency of the result on the initialisation [12]. Evidently, all these simplified assumptions did not make the SfS problem easier but actually rendered it more difficult from both a theoretical and a practical viewpoint.

This observation led to significant progress in the last few years. Nowadays, a perspective camera model [7, 13, 14] based on the inverse square law for light attenuation [12, 15] has become *the* standard assumption of recent SfS methods including those techniques with more advanced, i.e. non-Lambertian, reflection models [16, 17]. Moreover, with the consideration of the perspective camera model, the assumed position of the light source was moved from infinity to the optical centre of the camera [7]. While, this choice is very convenient from a computational viewpoint, it is obvious that a light source cannot be located at this place. This holds particularly for flash photography, where the position of the optical centre and the light source differ by construction.

In face of these considerations, it is surprising that there has hardly been any effort in the literature to model perspective SfS with an *arbitrary* position of the light source. In fact, there is only one work known to the authors, where a variational model for endoscopic SfS was proposed with a position of the light source different than the one in the optical centre [9]. This approach, however, suffers from two main drawbacks. On the one hand, the approach does not make use of proper discretisations of the hyperbolic terms such as e.g. upwind-type schemes [18]. This, however, would be necessary to ensure solutions in the viscosity sense [19]. On the other hand, the numerical algorithm proposed for this method is quite slow. In fact, the authors rely on a simple Jacobi-like scheme that is moreover explicit in the irradiance equation [20].

Contributions. In this paper we address all of the aforementioned problems. To this end, we formulate the perspective SfS problem in terms of a *Hamilton-Jacobi (HJE) equation* based on *spherical coordinates*. While such approaches have already been proposed for the standard case with the light source being located at the optical centre of the camera [15, 21], we demonstrate that employing such a spherical coordinate system is perfectly suited for the general case where the position of the light source can be arbitrary. In this context, our contributions are twofold:

1. On the modelling side, we derive a novel mathematical model for SfS in spherical coordinates which we call the *generalised brightness equation*. While the model itself can handle the most general geometry with the light source not being located in the optical centre of the camera, its compact and elegant structure suggests that this approach is the natural and intuitive way to formulate this problem.
2. On the numerical side, we develop a *highly efficient numerical algorithm* for solving the resulting highly non-linear HJE. This specifically tailored algorithm not only extends the popular fast marching (FM) method [22] by an iterative correction step but also guarantees to find solutions in the viscosity sense at the same time.

Summarising, we propose a perspective SfS approach that combines the applicability of a general SfS method with the efficiency of FM based approaches.

Organisation. In Section 2 we start by discussing the general perspective SfS framework. In Section 3 we then describe the representation of a surface in both Cartesian and the spherical coordinates. This allows us to compute the corresponding surface normal in Section 4 and finally to derive a compact formulation of the brightness equation for the general case. In Section 5. After we discuss our extended variant of the FM scheme in to solve this equation efficiently in Section 6, we present the results of our method in Section 7. The paper is concluded by a summary in Section 8.

2 Perspective Shape from Shading

Let us consider the general setting for perspective SfS with focal length f , where the position of the light source can be anywhere in the scene. Let us furthermore assume that the surface is Lambertian with uniform albedo and the light fall-off follows the inverse square law. Then, the brightness of the acquired image I is given by the so-called *brightness equation* [12]:

$$I(\mathbf{x}) = \frac{1}{r^2} \left(\frac{\mathbf{n}}{|\mathbf{n}|} \cdot \mathbf{L} \right). \quad (1)$$

Here, $\mathbf{x} = (x_1, x_2)^\top \in \Omega \subset \mathbb{R}^2$ denotes a pixel position in the rectangular image plane, \cdot the scalar product, \mathbf{L} the normalised light direction, \mathbf{n} the surface normal vector, $|\cdot|$ the Euclidean norm, and r the distance from the light source to the surface point.

Please note that in the literature this equation is typically parametrised such that the light source is located in the optical centre of the camera [12, 16, 17]. We will denote this specific variant of Eq. (1) as *restricted brightness equation*. In our approach, however, we follow a more general approach. We allow the light source to be everywhere in the image and parametrise the surface and thus the surface normal accordingly.

A sketch that illustrates the general scene geometry that comes with our model is depicted in Fig. 1. As one can see, w.l.o.g. we have chosen the origin of the coordinate system such that it coincides with the location of the light source. This decision will allow us to derive a mathematical model that is compact and elegant at the same time. As a first step towards this model, we have to parametrise the surface of the object

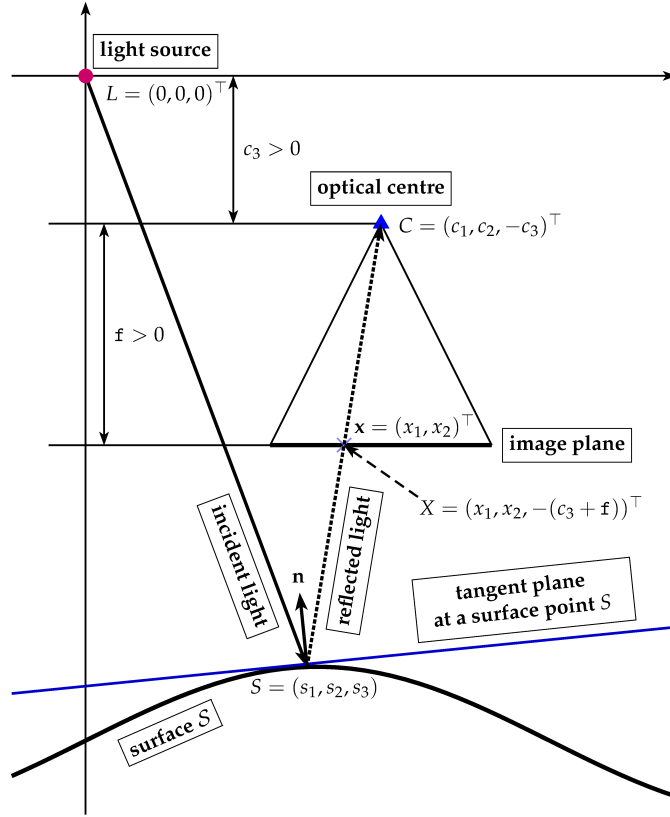


Fig. 1. Cross section of a 3-D model for perspective SfS with arbitrary position of the light source. The distance between the light source L and the point S on the surface is denoted by r in Eq. (1).

to compute the corresponding surface normal. This will be done in the next section. Afterwards we can derive the *general brightness equation* – the brightness equation that is parametrised such that it allows for an arbitrary position of the light source.

3 Parametrisation of the Surface

When it comes to the parametrisation of the object surface, recent SfS methods make use of standard Cartesian coordinates [9, 16, 17]. In the general case, however, such coordinates have one decisive drawback illustrated in Fig. 2(a) and Fig. 2(b): When the light source is not located in the optical centre of the camera, the *critical points*, i.e. the points of the object with largest local height, are not any longer the brightest points, i.e. the points that are closest to the light source. In short: Local intensity maxima do not identify critical points (local surface maxima). This is due to the fact that in SfS with Cartesian coordinates, the depth is measured along the x_3 -axis (Fig. 2: vertical axis).

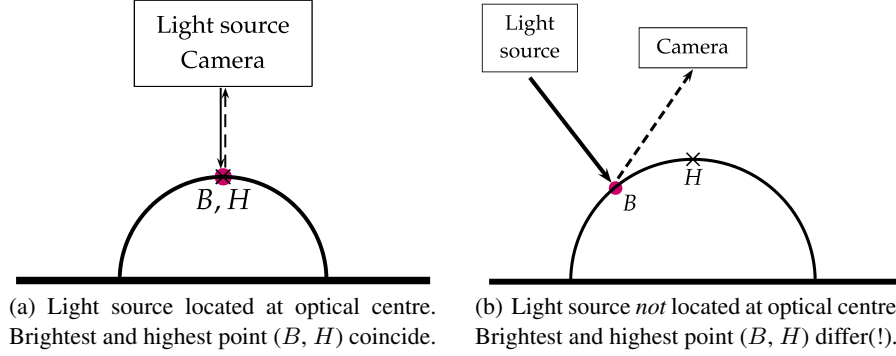


Fig. 2. Relationship between the brightest point B (critical point) and the highest point H of the object depending on the scene geometry. The problem of differing H and B is inherent to Cartesian coordinates. In a spherical coordinates with origin at the light source, B is always H .

Since identifying critical points is required to apply efficient algorithms of fast marching (FM) type [22–26] to solve the brightness equation in (1), we propose the following solution to the problem: By considering a *spherical coordinate system* with the origin placed at the position of the light source, we measure the depth and thus the critical points from the viewpoint of the light source. Per construction, in such a coordinate system, the locally brightest points in the image coincide again with the critical points. Please recall in this context that (i) the albedo is assumed to be uniform, (ii) surface normals at local maxima are parallel to the direction of incoming light (per definition of local maxima in our new coordinate system) and (iii) remaining convex-concave ambiguities are resolved by the light fall-off factor $1/r^2$ in the brightness equation [12].

Let us now describe our parametrisation. To this end, we start with standard Cartesian coordinates and then derive the corresponding formulation for the spherical case.

3.1 Surface Representation in Cartesian Coordinates

Considering Cartesian coordinates and following the notation from Fig. 1, the vector from the camera position C to a point X in the image plane is given by

$$\overrightarrow{CX} = \overrightarrow{LX} - \overrightarrow{LC} = \begin{bmatrix} x_1 \\ x_2 \\ -(c_3 + f) \end{bmatrix} - \begin{bmatrix} c_1 \\ c_2 \\ -c_3 \end{bmatrix} = \begin{bmatrix} x_1 - c_1 \\ x_2 - c_2 \\ -f \end{bmatrix}, \quad (2)$$

where \overrightarrow{AB} stands for a vector with starting point A and endpoint B . Furthermore we can use (2) to express the vector between the light source L and the surface point S

$$\begin{aligned} \overrightarrow{LS} &= \overrightarrow{LC} + \overrightarrow{CS} = \overrightarrow{LC} + \lambda \overrightarrow{CX} \\ &= \begin{bmatrix} c_1 \\ c_2 \\ -c_3 \end{bmatrix} + \lambda \begin{bmatrix} x_1 - c_1 \\ x_2 - c_2 \\ -f \end{bmatrix} = \begin{bmatrix} \lambda x_1 + (1 - \lambda) c_1 \\ \lambda x_2 + (1 - \lambda) c_2 \\ -(c_3 + \lambda f) \end{bmatrix} =: \begin{bmatrix} s_1 \\ s_2 \\ s_3 \end{bmatrix}, \end{aligned} \quad (3)$$

where $\lambda \in \mathbb{R}$ is a scaling factor that we are looking for. In particular, it holds that

$$|\overrightarrow{LS}|^2 = s_1^2 + s_2^2 + s_3^2 = [c_1 + \lambda(x_1 - c_1)]^2 + [c_2 + \lambda(x_2 - c_2)]^2 + (c_3 + \lambda f)^2. \quad (4)$$

In the following, we refrain from estimating the scaling factor λ , but solve for the distance $s_1^2 + s_2^2 + s_3^2$ from the light source to the surface directly. To this end, it turns out once again, that is advantageous to consider the problem in spherical coordinates.

3.2 Surface Representation in Spherical Coordinates

In order to express the distance from the light source to the surface in spherical coordinates, we have to define a suitable basis. Following Fig. 3, we represent the Cartesian vector \mathbf{r} via two angles θ and φ , respectively, as well as a radius r :

$$\mathbf{r} = R_{x_3}(\theta) R_{x_2}(\varphi) \begin{bmatrix} 0 \\ 0 \\ r \end{bmatrix} = \begin{bmatrix} \cos \theta \cos \varphi - \sin \theta \cos \theta \sin \varphi \\ \sin \theta \cos \varphi \cos \theta \sin \varphi \\ -\sin \varphi & 0 & \cos \varphi \end{bmatrix} \begin{bmatrix} 0 \\ 0 \\ r \end{bmatrix}. \quad (5)$$

Here, the two matrices

$$R_{x_3}(\theta) = \begin{bmatrix} \cos \theta & -\sin \theta & 0 \\ \sin \theta & \cos \theta & 0 \\ 0 & 0 & 1 \end{bmatrix}, \quad R_{x_2}(\varphi) = \begin{bmatrix} \cos \varphi & 0 & \sin \varphi \\ 0 & 1 & 0 \\ -\sin \varphi & 0 & \cos \varphi \end{bmatrix} \quad (6)$$

represent rotations around the x_3 - and x_2 -axis. The corresponding orthonormal basis is

$$\mathbf{e}_\varphi = \begin{bmatrix} \cos \varphi \cos \theta \\ \cos \varphi \sin \theta \\ -\sin \varphi \end{bmatrix}, \quad \mathbf{e}_\theta = \begin{bmatrix} -\sin \theta \\ \cos \theta \\ 0 \end{bmatrix}, \quad \mathbf{e}_r = \begin{bmatrix} \sin \varphi \cos \theta \\ \sin \varphi \sin \theta \\ \cos \varphi \end{bmatrix}, \quad (7)$$

where

$$\begin{bmatrix} \varphi \\ \theta \end{bmatrix} = \begin{bmatrix} \arccos \frac{s_3}{\sqrt{s_1^2 + s_2^2 + s_3^2}} \\ \arctan \frac{s_2}{s_1} \end{bmatrix}. \quad (8)$$

Thus, we can express the distance from the light source to the surface via the relation

$$\begin{bmatrix} s_1 \\ s_2 \\ s_3 \end{bmatrix} =: \mathbf{r} := r \mathbf{e}_r \quad \text{with} \quad r = \sqrt{s_1^2 + s_2^2 + s_3^2}. \quad (9)$$

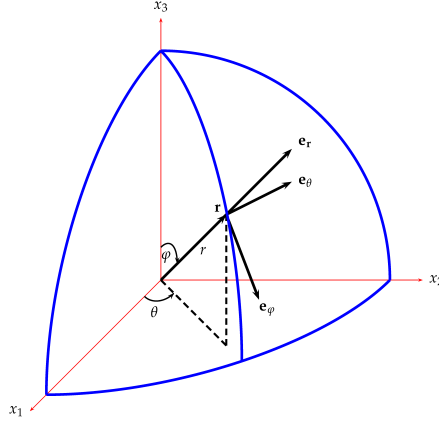


Fig. 3. The spherical system employed in this work. x_1 , x_2 and x_3 are conventional Cartesian coordinate axes. \mathbf{e}_r , \mathbf{e}_φ and \mathbf{e}_θ stand for basis vectors with respect to each direction in the spherical system. The distance between the light source L and the point S on the surface corresponds to r .

4 Computation of the Surface Normal

After we have parametrised the distance to the surface in spherical coordinates, we have to compute the *surface normal* for each pixel of the input image. This can be done by first determining the vectors defining the tangent plane – these vectors are given by the derivatives of the surface with respect to the two directions orthogonal to \mathbf{r} , namely θ and φ – and then by computing the cross product to obtain the corresponding normal vector. Using the definition of \mathbf{r} from (9), the surface normal is then given by

$$\begin{aligned}
 \mathbf{n} &= \frac{\partial (r\mathbf{e}_r)}{\partial \theta} \times \frac{\partial (r\mathbf{e}_r)}{\partial \varphi} \\
 &= \left(\frac{\partial r}{\partial \theta} \mathbf{e}_r + r \frac{\partial \mathbf{e}_r}{\partial \theta} \right) \times \left(\frac{\partial r}{\partial \varphi} \mathbf{e}_r + r \frac{\partial \mathbf{e}_r}{\partial \varphi} \right) \\
 &= \left(\frac{\partial r}{\partial \theta} \mathbf{e}_r \times \frac{\partial r}{\partial \varphi} \mathbf{e}_r \right) + \left(\frac{\partial r}{\partial \theta} \mathbf{e}_r \times r \frac{\partial \mathbf{e}_r}{\partial \varphi} \right) + \left(r \frac{\partial \mathbf{e}_r}{\partial \theta} \times \frac{\partial r}{\partial \varphi} \mathbf{e}_r \right) + \left(r \frac{\partial \mathbf{e}_r}{\partial \theta} \times r \frac{\partial \mathbf{e}_r}{\partial \varphi} \right) \\
 &= \frac{\partial r}{\partial \theta} \frac{\partial r}{\partial \varphi} \underbrace{(\mathbf{e}_r \times \mathbf{e}_r)}_{=0} + r \frac{\partial r}{\partial \theta} \left(\mathbf{e}_r \times \frac{\partial \mathbf{e}_r}{\partial \varphi} \right) + r \frac{\partial r}{\partial \varphi} \left(\frac{\partial \mathbf{e}_r}{\partial \theta} \times \mathbf{e}_r \right) + r^2 \left(\frac{\partial \mathbf{e}_r}{\partial \theta} \times \frac{\partial \mathbf{e}_r}{\partial \varphi} \right) \\
 &= r \frac{\partial r}{\partial \theta} \left(\mathbf{e}_r \times \frac{\partial \mathbf{e}_r}{\partial \varphi} \right) + r \frac{\partial r}{\partial \varphi} \left(\frac{\partial \mathbf{e}_r}{\partial \theta} \times \mathbf{e}_r \right) + r^2 \left(\frac{\partial \mathbf{e}_r}{\partial \theta} \times \frac{\partial \mathbf{e}_r}{\partial \varphi} \right) \\
 &\stackrel{(11)}{=} r \frac{\partial r}{\partial \theta} (\mathbf{e}_r \times \mathbf{e}_\varphi) + r \frac{\partial r}{\partial \varphi} (\sin \varphi \mathbf{e}_\theta \times \mathbf{e}_r) + r^2 (\sin \varphi \mathbf{e}_\theta \times \mathbf{e}_\varphi) \\
 &\stackrel{(12)}{=} r \frac{\partial r}{\partial \theta} \mathbf{e}_\theta + r \sin \varphi \frac{\partial r}{\partial \varphi} \mathbf{e}_\varphi - r^2 \sin \varphi \mathbf{e}_r.
 \end{aligned}$$

Thereby we used the following relations that hold by definition

$$\frac{\partial \mathbf{e}_r}{\partial \varphi} = \begin{bmatrix} \cos \varphi \cos \theta \\ \cos \varphi \sin \theta \\ -\sin \varphi \end{bmatrix} \stackrel{(\heartsuit)}{=} \mathbf{e}_\varphi, \quad \frac{\partial \mathbf{e}_r}{\partial \theta} = \begin{bmatrix} -\sin \varphi \sin \theta \\ \sin \varphi \cos \theta \\ 0 \end{bmatrix} \stackrel{(\heartsuit)}{=} \sin \varphi \mathbf{e}_\theta. \quad (11)$$

as well as the fact that $(\mathbf{e}_\varphi, \mathbf{e}_\theta, \mathbf{e}_r)$ constitutes a right-handed system, i.e. we have

$$\mathbf{e}_r \times \mathbf{e}_\varphi = \mathbf{e}_\theta, \quad \mathbf{e}_\varphi \times \mathbf{e}_\theta = \mathbf{e}_r, \quad \mathbf{e}_\theta \times \mathbf{e}_r = \mathbf{e}_\varphi. \quad (12)$$

5 Generalised Brightness Equation

After we have computed the surface normal, we are now in the position to set up the brightness equations for the general case. Following Eq. (1) this requires to evaluate the expressions $\mathbf{n} \cdot \mathbf{L}$ and $|\mathbf{n}|$. Based on Fig. 1, the light direction is given by

$$\mathbf{L} = -\mathbf{e}_r. \quad (13)$$

When plugging (10) and (13) into \mathbf{n} and \mathbf{L} , respectively, the dot product $\mathbf{n} \cdot \mathbf{L}$ becomes

$$\begin{aligned} \mathbf{n} \cdot \mathbf{L} &= \left(r \frac{\partial r}{\partial \theta} \mathbf{e}_\theta + r \sin \varphi \frac{\partial r}{\partial \varphi} \mathbf{e}_\varphi - r^2 \sin \varphi \mathbf{e}_r \right) \cdot (-\mathbf{e}_r) \\ &= r^2 \sin \varphi \end{aligned} \quad (14)$$

while the (squared) magnitude of the surface normal is given by the expression

$$|\mathbf{n}|^2 = \mathbf{n} \cdot \mathbf{n} = r^2 \left[\left(\frac{\partial r}{\partial \theta} \right)^2 + \sin^2 \varphi \left(\frac{\partial r}{\partial \varphi} \right)^2 + r^2 \sin^2 \varphi \right]. \quad (15)$$

In both cases we have exploited the orthonormality of the basis vectors; see Eq. (12). Using our results from (14) and (15) in Eq. (1) then gives the brightness equation

$$\begin{aligned} I &= \frac{1}{r^2} \left(\frac{\mathbf{n}}{|\mathbf{n}|} \cdot \mathbf{L} \right) \\ \Rightarrow r^2 I |\mathbf{n}| - \mathbf{n} \cdot \mathbf{L} &= 0 \\ \Rightarrow r^3 I \sqrt{\left(\frac{\partial r}{\partial \theta} \right)^2 + \sin^2 \varphi \left(\frac{\partial r}{\partial \varphi} \right)^2 + r^2 \sin^2 \varphi} - r^2 \sin \varphi &= 0 \\ \Rightarrow I \sqrt{\frac{1}{r^2 \sin^2 \varphi} \left(\frac{\partial r}{\partial \theta} \right)^2 + \frac{1}{r^2} \left(\frac{\partial r}{\partial \varphi} \right)^2 + 1} - \frac{1}{r^2} &= 0 \end{aligned} \quad (16)$$

We can further simplify this equation using the following relation:

$$\nabla r = \frac{1}{r} \left(\frac{\partial r}{\partial \varphi} \right) \mathbf{e}_\varphi + \frac{1}{r \sin \varphi} \left(\frac{\partial r}{\partial \theta} \right) \mathbf{e}_\theta. \quad (17)$$

Thus we finally obtain a very compact and elegant formulation that we will denote as *generalised brightness equation*. It is given by the Hamilton-Jacobi equation (HJE):

$$I \sqrt{|\nabla r|^2 + 1} - \frac{1}{r^2} = 0. \quad (18)$$

6 A Fast Marching Scheme for Spherical Coordinates

After we have derived the generalised brightness equation in the previous section, let us now discuss how it can be efficiently solved for the unknown radial distance field r (solved in the viscosity sense [24]). For this kind of HJEs so called fast marching (FM) schemes are among the fastest solvers in the literature [22–26]. Starting from critical points, such schemes are based on propagating the solution to the remaining points on the surface. Typically, each pixel is only visited once such that in the optimal case the performance is linear in the number of pixels [25]. Unfortunately, standard FM schemes cannot be applied in our case, since they have been designed for eikonal-type of the form $H(\cdot, \nabla r)$ without an explicit dependency on r . Moreover, our HJE is formulated in terms of spherical coordinates such that I actually depends on the solution r via the parametrised Cartesian pixel position $\mathbf{x} = (x(\theta, \varphi, r), y(\theta, \varphi, r))^\top$. Therefore, we propose the following specifically tailored variant of the FM scheme to solve our general HJE of type $H(\cdot, \nabla r, r)$ in spherical coordinates:

1. We identify critical points of the surface based on their brightness (cf. Section 3). Since their distance to the light source is minimal, we know that $\nabla r = 0$, which in turn allows us to solve Eq. (18) directly for the radial depth r .
2. The main task of the FM update process is to spread information from the critical points to the other points on the surface and update them solving Eq. (18). Since our HJE is highly nonlinear and depends on both r and ∇r , we apply the iterative strategy proposed in [17] in the context of nonlinear HJEs for Euclidean coordinates and solve (18) using the classical *regula falsi* method. Thereby, spatial derivatives are discretised using the standard upwind scheme [18]. Since our algorithm works in spherical coordinates, we propagate the information to neighbouring locations in terms of θ and φ rather than x and y . This also requires to evaluate the brightness values of the input image at subpixel locations, which is realised in terms of bilinear interpolation. Moreover, we need an additional *correction step*: Since the location to evaluate the image brightness depends on r (see above), we have to update this brightness value each iteration within our iterative regular falsi framework. The iterations are stopped, if the residual of the equation drops below a certain threshold.
3. We proceed to the adjacent locations in terms of θ and φ and solve (18) there. Although the parametrisation is different, the order in which the locations are traversed, is analogue to the Euclidean case (see [17] for details).

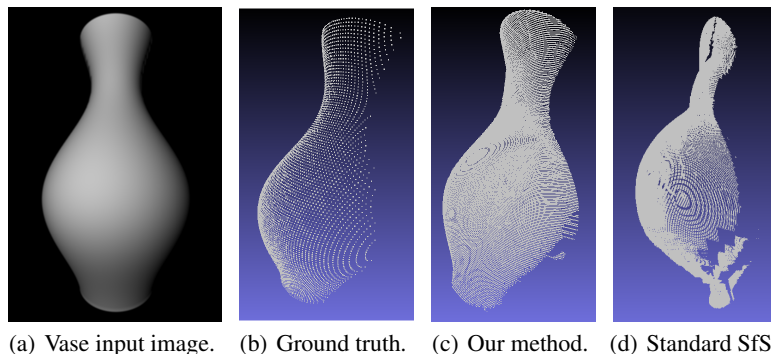


Fig. 4. The Vase experiment.

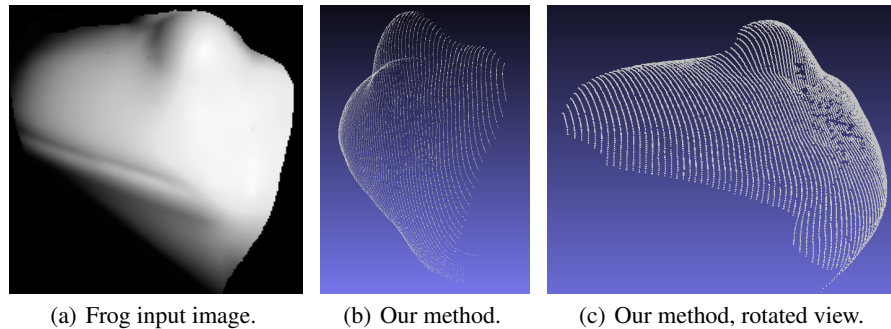
7 Experiments

Let us now evaluate our perspective SfS method for the general case. To this end, we have considered both a synthetic and a real-world image.

In our first experiment, we used our method to reconstruct the shape of a vase. The corresponding input image is depicted in Fig. 4(a). As one can see the light source is located in the upper left corner of the scene. The result obtained by our method as well as the ground truth are shown in Fig. 4(c) and Fig. 4(b), respectively. Evidently, the reconstructed shape looks very realistic. Moreover, in order to evaluate the impact of the general model on the reconstruction quality, we compared our result to the one of a perspective SfS method based on the restricted brightness equation, i.e. where the light source is assumed to be in the optical centre of the camera. As one can see from the corresponding result in Fig. 4(d), this method fails completely. This shows that the generalised brightness equation is essential for the success of SfS in practical applications – in particular if the assumption that the light source is close to the optical centre of the camera does not hold.

In our second experiment, we applied our perspective SfS technique for the general case to a real-world image. This image shows a sculpture that depicts the head of a frog (see Fig. 5(a)). This time, the light source is located in the right centre of the scene. Once again, we can see that the reconstruction looks reasonable. Thereby, we have to keep in mind that the head of the frog is reconstructed from the viewpoint of the light source. Moreover, this experiment shows nicely that the discrepancy between the position of the light source and the optical centre of the camera should not be too large. While the general model is capable of handling such situations, the overlap between both viewpoints may become quite small. In that case, the reconstruction will only show a very small part of the original object. In our experiment, however, the reconstructed part is still sufficiently large to give a good impression of the overall object surface.

The runtime of our approach is in the order of 40 seconds for a megapixel result, i.e. a reconstruction of size 1024×1024 . Please note that this runtime is not related to the size of the input image, but the angular sampling of the radial depth (i.e. of θ, φ).



(a) Frog input image.

(b) Our method.

(c) Our method, rotated view.

Fig. 5. The Frog experiment.

8 Summary

In this paper we proposed a novel model for perspective SfS for the general case. Unlike previous methods that restricted the position of the light source to be located in the optical centre of the camera, our model allows the light source to be placed anywhere in the scene. In this context, a formulation of the problem as Hamilton-Jacobi equation in terms of spherical coordinates turned out to be very useful: On the one hand, it allowed us to formulate the brightness equation for the complex general case in a very compact and elegant way. On other hand, it enabled us to determine critical points and thus to develop a specifically tailored variant of the highly efficient FM scheme as solver for our model. Experiments have shown that our method works well in practice and that it gives reconstructions of good quality. It even allows to obtain results in those cases where standard models based on the restricted brightness equation fail. This shows that considering alternative parametrisations can be worthwhile in many computer vision problems. They may turn an originally difficult problem into a simple one - from both a modelling and a numerical viewpoint.

Acknowledgements. This work has been partly funded by the Deutsche Forschungsgemeinschaft (BR 2245/3-1, BR 4372/1-1). Moreover, Silvano Galliani gratefully acknowledges funding by the Fraunhofer Institute for Industrial Mathematics (ITWM).

References

1. Rindfleisch, T.: Photometric method for lunar topography. *Photogrammetric Engineering* **32** (1966) 262–277
2. Horn, B.K.P.: Shape from shading: a method for obtaining the shape of a smooth opaque object from one view. PhD thesis, Massachusetts Institute of Technology (1970)
3. Ostrov, D.N.: Viscosity solutions and convergence of monotone schemes for synthetic aperture radar shape-from-shading equations with discontinuous intensities. *SIAM Journal on Applied Mathematics* **59** (1999) 2060–2085
4. Bors, A.G., Hancock, E.R., Wilson, R.C.: Terrain analysis using radar shape-from-shading. *IEEE Transactions on Pattern Analysis and Machine Intelligence* **25** (2003) 974–992

5. Abdelrahim, A.S., Abdelrahman, M.A., Abdelmunim, H., Farag, A., Miller, M.: Novel image-based 3D reconstruction of the human jaw using shape from shading and feature descriptors. In: *Proceedings of the British Machine Vision Conference*. (2011) 1–11
6. Okatani, T., Deguchi, K.: Shape reconstruction from an endoscope image by shape from shading technique for a point light source at the projection center. *Computer Vision and Image Understanding* **66** (1997) 119–131
7. Tankus, A., Sochen, N., Yeshurun, Y.: Perspective shape-from-shading by fast marching. In: *IEEE Conference on Computer Vision and Pattern Recognition*. Volume 1. (2004) 43–49
8. Wang, G.H., Han, J.Q., Zhang, X.M.: Three-dimensional reconstruction of endoscope images by a fast shape from shading method. *Measurement Science and Technology* **20** (2009)
9. Wu, C., Narasimhan, S., Jaramaz, B.: A multi-image shape-from-shading framework for near-lighting perspective endoscopes. *International Journal of Computer Vision* **86** (2010) 211–228
10. Zhang, R., Tsai, P.S., Cryer, J.E., Shah, M.: Shape from shading: A survey. *IEEE Transactions on Pattern Analysis and Machine Intelligence* **21** (1999) 690–706
11. Durou, J.D., Falcone, M., Sagona, M.: Numerical methods for shape-from-shading: A new survey with benchmarks. *Computer Vision and Image Understanding* **109** (2008) 22–43
12. Prados, E., Faugeras, O.: Shape from shading: A well-posed problem? In: *IEEE Conference on Computer Vision and Pattern Recognition*. (2005) 870–877
13. Courteille, F., Crouzil, A., Durou, J.D., Gurdjos, P.: Towards shape from shading under realistic photographic conditions. In: *IEEE International Conference on Pattern Recognition*. Volume 2. (2004) 277–280
14. Tankus, A., Sochen, N., Yeshurun, Y.: Shape-from-shading under perspective projection. *International Journal of Computer Vision* **63** (2005) 21–43
15. Bruvoll, S., Reimers, M.: Spherical surface parameterization for perspective shape from shading. *Pattern Recognition Letters* **33** (2012) 33–40
16. Ahmed, A., Farag, A.: A new formulation for shape from shading for non-Lambertian surfaces. In: *IEEE Conference on Computer Vision and Pattern Recognition*. (2006) 1817–1824
17. Vogel, O., Breuß, M., Weickert, J.: Perspective shape from shading with non-Lambertian reflectance. In: *DAGM Symposium on Pattern Recognition*. (2008) 517–526
18. Rouy, E., Tourin, A.: A viscosity solutions approach to shape-from-shading. *SIAM Journal on Numerical Analysis* **29** (1992) 867–884
19. Crandall, M., Lions, P.L.: Viscosity solutions of Hamilton-Jacobi equations. *Transactions of the American Mathematical Society* **277** (1983) 1–42
20. Horn, B., Brooks, M.: The variational approach to shape from shading. *Computer Vision, Graphics, and Image Processing* **33** (1986) 174–208
21. Alkhalifah, T., Fomel, S.: Implementing the fast marching eikonal solver: spherical versus Cartesian coordinates. *Geophysical Prospecting* **49** (2001) 165–178
22. Sethian, J.: A fast marching level set method for monotonically advancing fronts. In: *Proc. of the National Academy of Sciences of the United States of America*. (1995) 1591–1595
23. Sethian, J.: Fast-marching level-set methods for three-dimensional photolithography development. In: *Proc. SPIE, Optical Microlithography IX*. Volume 2726., (1996) 262–272
24. Sethian, J.: *Level set methods and fast marching methods*. Cambridge University Press (1999)
25. Tsitsiklis, J.: Efficient algorithms for globally optimal trajectories. *IEEE Transactions on Automatic Control* **40** (1995) 1528–1538
26. Helmsen, J., Puckett, E., Colella, P., Dorr, M.: Two new methods for simulating photolithography development in 3D. In: *Proc. SPIE, Optical Microlithography IX*. Volume 2726., (1996) 253–261